Metalloporphyrines as Active Site Analogues—Lessons from Enzymes and Enzyme Models

WOLF-D. WOGGON
Department of Chemistry, University of Basel, St. Johanns-Ring 19, CH-4056 Basel, Switzerland

Received August 27, 2004

ABSTRACT
Research at the interface of enzyme chemistry and organic chemistry of metal complexes is particularly rewarding employing metal porphyrins as cofactor surrogates. Three examples are discussed: active site analogues of cytochrome P450 and chloroperoxidase (CPO), both heme-thiolate proteins, and enzyme models of β-carotene monooxygenase, a non-heme iron protein. In all cases, catalytically active synthetic systems could be established displaying chemical reactivity close to the native proteins. Further, it is demonstrated that enzymatic reaction mechanisms can be elucidated by means of active site analogues (CPO) and information can be obtained from enzyme models that is useful to explain certain aspects of Nature's sophisticated approach to develop very efficient catalysts.

Introduction

The synthesis of enzyme models is a formidable challenge to the organic and bioinorganic chemist to establish a system that is structurally equivalent to the cofactor of the respective protein. Under ideal circumstances, the synthetic mimic not only is a structural analogue exhibiting spectroscopic features close to the enzyme's cofactor but also displays a similar reactivity and catalysis with decent turnover. Again, under ideal conditions catalytically competent intermediates can be identified and even the complete catalytic cycle may be reproduced.

It may be useful to distinguish active site analogues from enzyme models/mimics; the former notion reflects a very close structural similarity/identity to the cofactor, and the second term rather defines a system that is structurally more or less remote but displays similar reactivity/catalysis. In any case, investigations of synthetic cofactor surrogates is complementary to studies of the native protein such as X-ray structural analysis, site-directed mutagenesis, the determination of kinetic parameters, and isotope effects. Often information that cannot be obtained using the native protein becomes available employing suitable active site analogues, and finally this approach can lead to catalytic systems that are synthetically useful.

Wolf-D. Woggon received degrees in chemistry and geology from the Freie Universität Berlin and a Ph.D. in chemistry from the University of Zurich working under the direction of the late Hans Schmid. After a postdoctoral position with Sir Alan Battersby at the University of Cambridge, he returned to Zurich to complete his habilitation. In 1995, he joined the faculty of the University of Basel where he is currently a Professor of Chemistry and Head of the Department. The research of his group focuses on the enzymolgy of proteins that catalyze unusual reactions and the synthesis of functional enzyme models.

10.1021/ar0400793 CCC: $30.25
Published on Web 01/15/2005

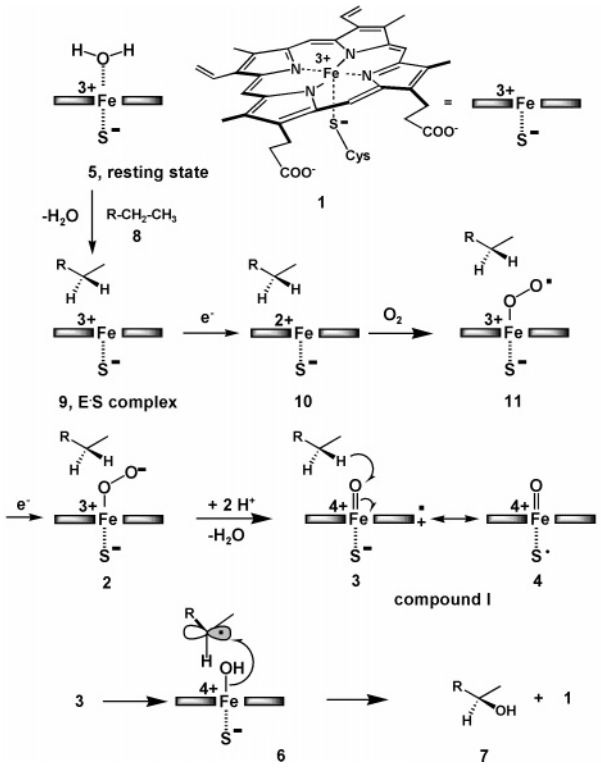

FIGURE 1. Catalytic cycle of cytochrome P450.

Due to the rich and well explored chemistry of metal porphyrins in particular, enzymes that contain these complexes as cofactors have long been attractive targets. In the present Account, we wish to report a few of our own contributions to metalloenzyme chemistry within the context of the respective area of protein chemistry and enzyme model chemistry.

II. Heme-Thiolate Proteins—Active Site Analogues of Cytochrome P450

Heme-thiolate proteins comprise abundant enzyme families such as cytochromes P450,[1] NO-synthases,[2−4] and chloroperoxidases (CPO). The first two proteins are extremely important to mammals due to their central role in metabolism of drugs/synthesis of hormones and the production of •NO as a signal messenger, respectively. In contrast, CPO has attracted attention mainly due to its diverse reactivity and versatility[5] and its particular reaction mechanism/conditions.[6]

These enzymes catalyze a surprisingly large repertoire of oxidation reactions even though their active sites are characterized by the same center of chemical reactivity, an iron protoporphyrin(IX) complex, **1**, bound to the protein via ionic interactions of the two propionate side chains and a thiolate ligand from a cysteine coordinating to the iron from the proximal site (Figure 1).

Our understanding of the complicated reaction pathways of heme-thiolate proteins[1,7,8] (Figure 1) rests to a large extent on investigations of cytochrome $P450_{cam}$, which catalyzes the hydroxylation of camphor at the 5-*exo* position and, hence, is the paradigm of the oxidation of

nonactivated C-atoms, one of the most remarkable reactions in nature. This cytosolic protein can be easily purified from *Pseudomonas putida* and has been overexpressed in other bacteria.[9] X-ray structures of various forms of $P450_{cam}$[10−15] have been obtained, as well as Laue snapshots[16] of certain intermediates. Numerous mechanistic studies and investigation of structurally remote model compounds established a sequence of events in the catalytic cycle of cytochrome P450, which is well defined up to intermediate **2**[17] (Figure 1).

The consecutive steps, though lacking definitive characterization, were deduced from studies using point-mutated enzymes and by comparing spectroscopic parameters of enzymes/model compounds and measuring isotope effects. In agreement with data from different sources is the formation of a high-valent iron(IV) oxo porphyrin radical cation intermediate, **3**, formed by protonation of the peroxo complex **2** and subsequent O−O bond cleavage. By analogy with model studies,[1] this intermediate is believed to have the electronic structure **3**[18] rather than **4**.[19] For the past 2 decades, the mechanism of P450-catalyzed hydroxylations was described as a two-step reaction of **3** with the substrate: hydrogen abstraction by the iron-oxo of **3** gives a substrate alkyl radical that is immediately trapped by $HO^{\bullet}$ from the iron, see **6**, yielding the hydroxylated substrate **7** and the water-free form of the enzyme's resting state, **1**. Several aspects of the catalytic cycle have been questioned, such as (i) the origin of the low-spin state of **5**,[20,21] the resting state of $P450_{cam}$, (ii) the electronic nature of compound I, **3**/**4**[1,18,19], (iii) the two-step oxygen-rebound mechanism,[22−24] and (iv) the significance of the unique thiolate ligand, which has been a matter of debate[25] since cytochrome 450 was discovered 40 years ago.[26]

Obviously three steps of the reaction sequence (Figure 1) are redox-sensitive: (i) reduction of iron(III) **9** → iron(II) **10**, (ii) addition of an electron to the terminal oxygen bound to iron, see **11** → **2**, and (iii) the interaction of **3**/**4** with the substrate. The redox potential of **3**/**4** can be estimated to be 1.3 V,[27] and hence, this intermediate not only can abstract $H^{\bullet}$ from substrates but can accept electrons from suitable substrates such as amines.[1] The transformation of **11** → **2** is required to initiate oxygen cleavage, and it is known in certain cases that the donation of the electron to **11** is a rate-limiting step leading to small, not fully expressed k_H/k_D for $H^{\bullet}$ removal,[1] as for the hydoxylation of camphor.

The six-coordinate resting state of $P450_{cam}$ **5** is an important intermediate of the catalytic cycle because its E_0 is held at negative values ($E_0 = -290$ mV)[28] due to the presence of the thiolate ligand. Hence acceptance of electrons from NADPH via putidaredoxin (Pdx, $E_0 = -235$ mV)[29,30] is thermodynamically disfavored. Further, electron-transfer rates from Pdx → **5** might be much slower than those for Pdx → **9** due to a difference of reorganization energy, λ, for electron transfer to the two spin states.[31,32] Thus, only the conversion of **5** to the high-spin iron(III) complex **9** ($E_0 = -170$ mV) yields an intermediate that can initiate the catalytic cycle. It is important to note that

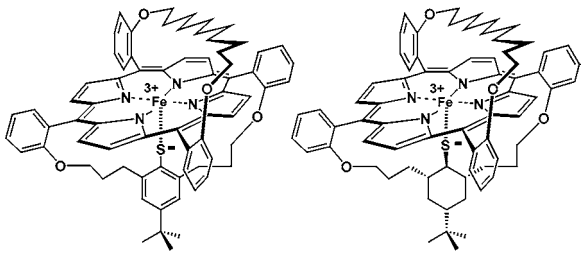

12 **13**

FIGURE 2. Active site analogues of cytochrome P450.

putidaredoxin (Pdx) can be replaced by other reducing agents for the transformation of **9** → **10** but the redox protein is indispensable for injection of the second electron, see **11**→ **2**, and in particular for catalytic turnover. The fact that **9** has the same E_0[28] whether or not Pdx is bound suggests that reorganization energy (λ_{total}) is not a driving force for electron-transfer Pdx → **9**. In contrast, addition of the second electron, Pdx → **11**,[33] is associated with a significant contribution of λ. Experiments with a (L358P)-$P450_{cam}$ mutant[34,35] revealed significant structural changes at both the distal and the proximal site indicating that this mutant serves as a structural and functional model for Pdx-bound $P450_{cam}$. Accordingly, binding of Pdx to $P450_{cam}$ may cause removal of one H-bond to the thiolate, see below, rendering the ligand a better π-donor and supporting O−O bond cleavage of the protonated form of **2**. This may have also consequences for the spin distribution in compound I, **3** ↔ **4**, and hence its reactivity.[24]

This fine-tuning of E_0 of **5** to −290 mV, one of the most elegant examples of gating biological electron transfer, is accomplished by two factors: (i) the iron(III) adopts a low-spin state, and (ii) the thiolate ligand provided by the cysteine is hydrogen-bonded to three amino acids of the protein backbone.[36] The latter aspect, not immediately observed in the first X-ray structures of $P450_{cam}$, was predicted from the E_0 values of our synthetic active site analogues **12** and **13** (Figure 2) displaying both significantly negative redox potentials (−607 and −714 mV) and indicating a clear correlation between E_0 and the effective charge at S^-.[37,38]

There are several possibilities for designing catalytic enzyme models having E_0 values close to those of $P450_{cam}$ or CPO ($E_0 = -140$ mV).[39] The synthetically most convenient way seems to be the preparation of electron-deficient porphyrins, such as **14** and **15** (Figure 3), which contain two *meso*-dichlorophenyl and two *meso*-pentafluorophenyl substituents, respectively. Porphyrin **14** exhibits $E_0 = -460$ mV[40] and **15** a redox potential of $E_0 = -134$ mV,[41] well within the range of E_0 values of CPO and P450.

From these model studies, it was concluded that the E_0 value is largely dependent on the electron-donating character of the proximal RS^-, see **12**/**13**, and the porphyrin ligand and modulated by substituents protecting the distal site of the porphyrin. It is interesting to note that ΔE_0 between **12** and **16**[42] (Figure 4) is about 100 mV, suggesting a E_0 dependence on the polarity of the distal

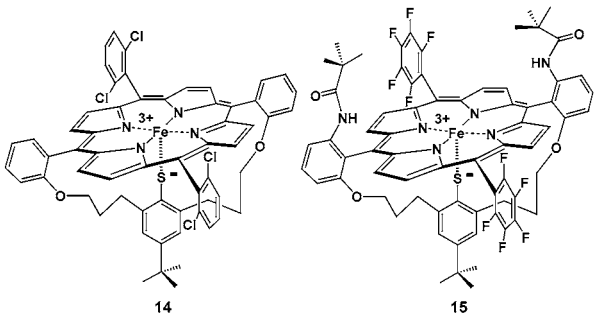

FIGURE 3. Electron-deficient iron(III) porphyrins.

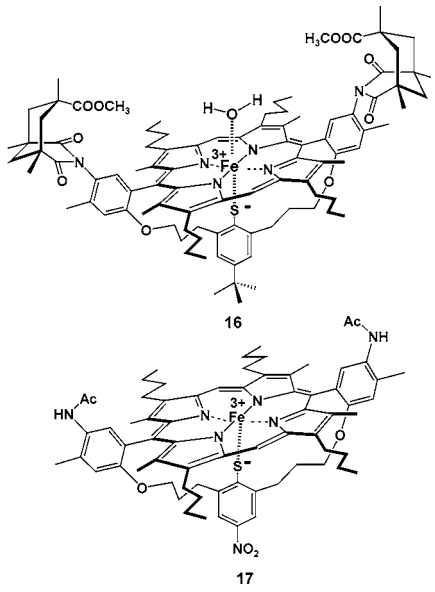

FIGURE 4. Synthetic iron(III) porphyrins with distinct proximal and distal coordination sites.

site. Only if the electron density at RS^- is reduced, see **17**,[43] or the electron donation from the porphyrin ligand is smaller, remarkable anodic shifts are observed. The main contribution to ΔE_0 of ca. +400 mV between the enzyme's resting state and its model compounds **12** and **13** can be attributed to the H-bonding to RS^- (e.g., of cysteine 357 in $P450_{cam}$). The important 120 mV anodic shift **5** → **9**, however, is associated with the change of the low-spin to the high-spin state. Though analogues have been prepared ($E_0 = -350$ mV) mimicking the unique $S^-_{cys}\cdots H-N$ bonding of $P450_{cam}$, these models are unsuitable for catalytic reactions.[44]

A third possiblity to approach the redox potential of the heme-thiolate proteins is a convenient variation of the thiolate ligand → SO_3^- (Figure 5). In agreement with our expectation the distribution of one negative charge at RS^-, over a much larger space volume at RSO_3^-, gave a very significant anodic shift of 285 mV to $E_0 = -175$ mV, see **18**, which, within experimental error, corresponds exactly to the value of **9**, the high-spin E·S complex of cytochrome $P450_{cam}$.

Interestingly, this unusual modification of the heme-thiolate model system produced a good catalytic system for epoxidations in the presence of PhIO with turnover up to 1500. The results of density functional theory (DFT) calcuations indicated that coordination of the RSO_3^- group

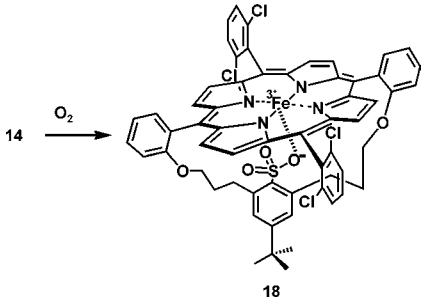

FIGURE 5. A new class of P450 enzyme models carrying a RSO_3^- ligand.

to the Fe center occurred through one oxygen donor and further indicated that the reaction pathways for an oxo iron(IV)−$^-$S−R porphyrin radical cation and an oxo iron-(IV)−$^-$OSO$_2$−R porphyrin radical cation are very similar with respect to allylic hydroxylation and epoxidation.[40]

The crystal structure of the resting state of cytochrome $P450_{cam}$ revealed that the substrate binding pocket is occupied by a cluster of six hydrogen-bonded water molecules, one of which coordinates to iron as sixth ligand.[11] Surprisingly, the resting state is predominantly low-spin and changes to a high-spin system when the camphor substrate binds and the water cluster is completely removed. Thus spin state changes are a significant factor in regulating the catalytic cycle of P450s, and furthermore, it can be assumed to trigger the mode/reactivity of oxygen insertion by $O{=}Fe^{IV}(porph^{+\bullet})(CysS^-)$ (compound I).[24]

To explain the origin of the low-spin character of the resting state of $P450_{cam}$, it can be speculated that the coordinating water molecule is polarized through the hydrogen-bonding network in the water cluster yielding a distinctive hydroxide character and hence a low-spin complex. On the other hand, semiempirical calculations suggested[21] a significant contribution of the electrostatic field of the surrounding protein, which stabilizes the low-spin resting state. By comparison of simulated and experimental ^{17}O electron spin echo envelope modulation (ESEEM) and pulsed electron nuclear double resonance (ENDOR)/four-pulse ESEEM spectra of the resting state of $P450_{cam}$, it has been concluded that the distal ligand is a water molecule rather than a hydroxide ligand.[45]

Using various electron paramagnetic resonance (EPR) techniques, we have shown that active site analogues $H_2O-Fe(III)(porph)(ArS^-)$, such as **16** (Figure 4), are definitely high-spin and only change to the low-spin state if the coordinating water is replaced by 1,2-dimethyl imidazole.[46] These results clearly indicated that the coordination of water to Fe(III) of the heme thiolate cofactor is insufficient to stabilize the low-spin state of the resting state of $P450_{cam}$. Accordingly, we designed the active site analogues **19** and **20**[47,48] (Figure 6) to distinguish experimentally between two effects: (i) the hydroxide character of the coordinating water and (ii) the contribution of the protein's electrostatic field. In this context, some structural features of **19** and **20** are worth noting, such as the sterically congested S^- ligand coordinating to Fe(III) and a crown ether capping the distal face of the porphyrin.

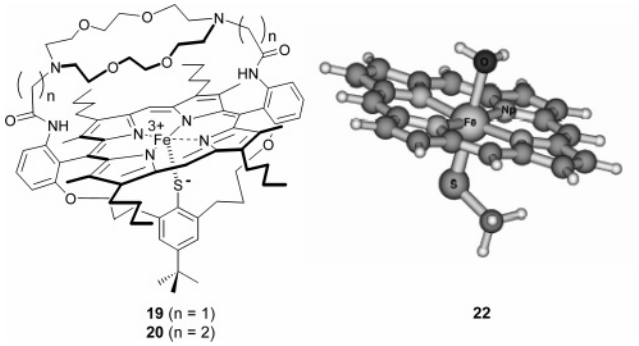

FIGURE 6. Crown-capped heme-thiolate enzyme models.

The 1,10-diaza-18-crown-6 is known to bind divalent cations such as Ba^{2+} and hence allows an investigation into the electrostatic field effect. Moreover, the oxygens of the crown ether can act as H-bond acceptors to water[49] coordinating to iron if placed at a proper distance. In contrast to **20**, hydrogen bonding is possible in **19**, and hence, in the latter, the diazacrown cap should mimic a possibly polarized water cluster in $P450_{cam}$ and a OH^--like character of the coordinating water molecule, respectively.

Synthetic complexes **19** and **20** showed characteristic UV−vis (λ_{max}(toluene) = 404 and 406 nm, respectively) and electrospray ionization mass spectrometry (ESI-MS) spectra (m/z 1469 $[M + Na]^+$ and m/z 1497 $[M + Na]^+$, respectively). In dry toluene, both **19** and **20** showed continuous wave (cw)-EPR spectra characteristic of pure high-spin iron porphyrins with a strong rhombic contribution from the ligand field. The EPR spectrum of **20** in water-saturated toluene was identical with the spectrum in dry toluene. In contrast, when **19** was measured in water-saturated toluene, low-spin signals in the EPR spectrum were obtained supporting the formation of **21**. These g-values are very similar to those obtained for the low-spin resting state of $P450_{cam}$ ($g = 2.45, 2.26, 1.91$).[1] In addition, we have already shown that the same low-spin signals ($g = 2.45, 2.23, 1.91$) can be obtained quantitatively, if an enzyme model with an open distal face is treated with an excess of 1,2-dimethyl imidazole, a strong ligand known to yield a pure low-spin complex.[46] The cw-EPR spectra recorded at 4 K were identical with spectra at 100 K except that the signals were sharper at lower temperature.

Thus it was concluded that water binds to the central metal of **21** and forms two hydrogen bonds with crown ether oxygens. The incomplete conversion of the high-spin state of **19** to the low-spin form **21** can be explained by the small excess of water present in toluene (∼3−4 equiv). Since binding of Ba^{2+} to **19** gave no change of spin state, an electric field component seemingly does not contribute to the stabilization of the low-spin form of the resting state model.

These results were supported by DFT calculations for which **22** was used as a model for **19** and **23** as a model for **21** (Figure 7). In **22**, the optimized structure of the low-spin state is favored by only 2.5 kcal mol^{-1} over the high-spin state. For H-bonding of the water molecule as in **21**,

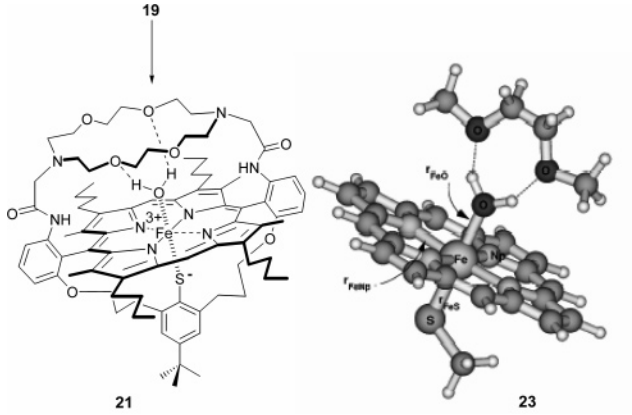

FIGURE 7. Water binding to complex **19**.

the low-spin state was unambiguously lower in energy by 7.2 kcal mol^{-1} compared to the high-spin state. H-bonding of the ether oxygens resulted in a significant change of the negative nuclear charge on the oxygen atom of the coordinated water molecule in the low-spin case (−0.86 for **22** to −0.91 for **23**) and in the high-spin case (−0.89 for **22** to −0.97 for **23**). The calculations were validated by comparison of the optimized structures with results from X-ray experiments. In fact, structural parameters r_{FeS}, r_{FeO}, r_{FeNp}, and d(Fe−porph. plane) obtained for **22** and **23** agree all within 0.1 Å with experimental values for the $P450_{cam}$ resting state[11] and the corresponding E·S complex.[12] Taken together, experiments and calculations support the view that polarization in the water cluster plays an important role for the observed low-spin resting state of $P450_{cam}$.

III. Heme-Thiolate Proteins—Active Site Analogues of Chloroperoxidase (CPO)

CPO, first isolated from the mold *Caldariomyces fumago*,[50] is the most versatile of the heme-thiolate enzymes, catalyzing the chlorination of activated C−H bonds employing H_2O_2 and Cl^- at pH 2.7 and reactions reminiscent of peroxidases, catalase, and cytochrome P450.[5] Despite numerous investigations of the enzyme, the identification of significant reactive intermediates remained elusive, and it was assumed that compound I oxidizes Cl^- and releases HOCl into solution, which in turn reacts with activated substrates RH in a nonenzymatic way.[51]

Through a combination of experiments with synthetic model compounds and with the enzyme chloroperoxidase, we obtained insight into the reaction pathway of CPO.

It was shown that **24** forms stable $^-$OCl and HOCl adducts, **25** and **26** (Figure 8) under strictly defined conditions,[52] and it was further demonstrated that only **26** is catalytically active to chlorinate monochlorodimedone, **27**, the substrate of the standard assay of CPO, yielding dichlorodimedone, **28**. It is important to note that **25**, and subsequently **26**, was produced from **24** by two independent reaction pathways, namely, using benzyl triethylammoniumhypochlorite[52] and H_2O_2, together with benzyl triethylammoniumchloride. In particular, the latter enzyme-like conditions suggested that **25** and **26** are

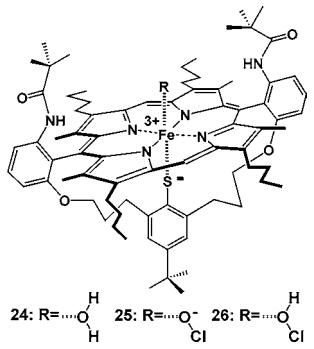

FIGURE 8. Active site analogues of CPO.

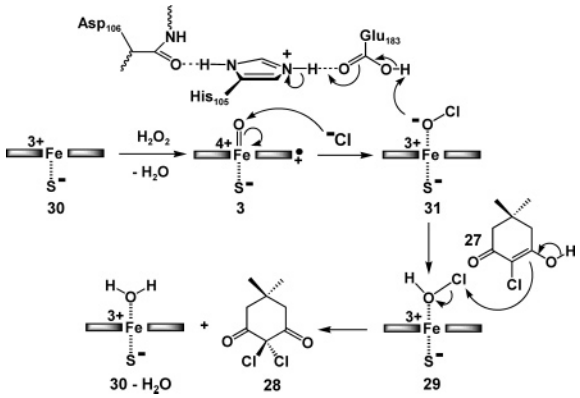

FIGURE 9. Proposed catalytic cycle of CPO.

kinetically competent analogues of intermediates of the catalytic cycle of the enzyme CPO. Consequently, the spectroscopic parameters of the active site analogues **25** and **26** were employed to search for these until then elusive intermediates of CPO's reaction sequence.

UV/vis spectroscopy of CPO from *Caldariomyces fumago* in the presence of NaOCl at a pH range of 3−9 revealed that only at pH 4.4 a new compound was detected.[53] This complex was identified as the HOCl adduct **29** of the active site's iron(III) porphyrin due to its split Soret band (λ_{max} = 376 and 434 nm) corresponding to the model complex **26** (λ_{max} = 388 and 416 nm). Taking information from the X-ray analysis of CPO's resting state **30** from *Caldariomyces fumago*, which identified three amino acid residues, Glu183, His105, and Asp106, above the porphyrin face opposite to the thiolate coordination site,[54] we concluded that these amino acids participate in catalysis as a proton delivery system (i) by assisting the hydrogen peroxide cleavage, leading to compound I, see **3**, and (ii) by protonation of the adduct **31** (Figure 9). Thus we assumed that the $^{-}$OCl adduct **31** would be observable only if the proton supply is inactivated. This was accomplished by covalent modification of His105 using diethylpyrocarbonate, which inactivates the catalytic activity of CPO completely.[55] In fact using this "CPO-derivative", we detected the −OCl adduct **31** of the heme-thiolate cofactor exhibiting a single Soret band (λ_{max} = 406 nm) close to the absorption of the corresponding complex **25** derived from the enzyme model **24**.[51]

Iron(III) porphyrins **24** and **25**/**26** served as a decisive guide to track intermediates of the catalytic cycle of CPO. Accordingly in model reactions, **26** is the Cl^{+} donor, but whether this is also true for **29**, the corresponding enzymatic intermediate, is debatable. HOCl may dissociate from **29** and diffuse to a substrate binding pocket where stereospecific chlorination could occur. This reaction, for example, could first involve the reaction of HOCl with the N^{ϵ} amino group of a lysine; the resulting chloramine could then serve as the chlorination agent for the bound substrate. Until now a binding site for halogenation has not been found, and a binding site for epoxidation has been only suggested by docking experiments.[56]

Complexes such as **24** have a certain limitation concerning stability and turnover when used in catalytic chlorinations. Thus we employed the *face-protected*, more reactive iron porphyrin **15** (Figure 3).[41] The complex **15** is an iron(III) high-spin (g = 6.318, g = 2.019) porphyrin displaying a Soret band in UV/vis spectroscopy at λ_{max} = 416 nm for Br^{-} as the sixth ligand and λ_{max} = 420 nm for the water complex. In comparison to the porphyrin **24** (λ_{max} = 408 nm, λ_{max} = 400 nm [Br^{-}]) the Soret band of **15** is considerably red-shifted due to the presence of the electron-withdrawing pentafluoro residues. Reduction of **15** with $NaBH_4$ in THF quantitatively provided the corresponding iron(II) complex with λ_{max} = 426 nm, which on addition of CO displayed the expected bathochrome shift to λ_{max} = 448 nm, characteristic of a heme-thiolate system and all other model compounds we prepared.

Thus regarding spectroscopy and electrochemistry, complex **15** is a suitable model to mimic different features of heme-thiolate proteins. With respect to chemical reactivity and stability, we have found that in the presence of benzyl triethylammoniumhypochlorite and H_2O_2, catalyst **15** retains about 85% of its activity within 1 h at room temperature, whereas the iron porphyrin **24** is completely oxidized. Brominations and chlorinations of activated C−H bonds using Bu_4NOBr/Bu_4NOCl and 0.05−0.09 mol % **15** (with acid or Lewis acid) gave turnovers of up to 1530. Accordingly, these experiments with synthetic CPO active site analogues not only revealed a reasonable reaction mechanism of the enzyme chloroperoxidase but also led to a catalytic system with appreciable turnover.[41]

IV. Carotene Monooxygenase—Reaction Mechanism and Enzyme Models

β-Carotene **32** is the parent structure and most important compound of the "orange pigments of life" comprising >650 carotenoids, which are abundant in photosynthetic bacteria and in the plant and animal kingdom. Both plants and bacteria can biosynthesize carotenoids,[57,58] but mammals rely on extraction from their diet. The significance of β-carotene **32** to humans concerns its antioxidant activity[59] and its enzymatic conversion to retinal **33** (provitamin A). To date, two modes of cleavage of **32** have been proposed: the *central cleavage* providing 2 mol of **33**,[60] and the more recently discovered *excentric cleavage*, which yields first apocarotenals, such as **34**, which may be degraded to **33** (Figure 10).[61]

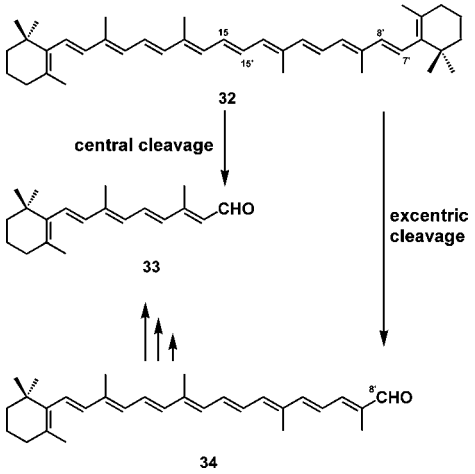

FIGURE 10. Central and excentric cleavage of β-carotene **32**.

Central cleavage of **32** seems to be the most important metabolic pathway, and enzymatic activity has been detected in various tissues since its discovery in the mid-1950s. Since then many attempts failed to purify and charcterize this enzyme. Nevertheless and despite the lack of definitive information regarding the enzymatic reaction mechanism, as well as the nature of the cofactor, the enzyme was termed β-carotene 15,15′-dioxygenase (EC 1.13.11.21).

We have been able to establish a purification protocol for the enzyme isolated from chicken intestinal mucosa, which led to the identification of the catalytically active protein.[62,63] Sequencing and expression of the hexa-His-tagged protein in *Escherichia coli* and BHK (baby hamster kidney) cells gave, after affinity chromatography, a catalytically active, cytosolic enzyme (60.3 kDa), which cleaves β-carotene **32** to retinal **33** as the only reaction product.

Iron was identified by atomic emission spectroscopy using an inductively coupled high-frequency plasma (IPC) as the only metal ion associated with the (overexpressed) protein in a 1:1 stoichiometry, and since a chromophore is absent in the protein, heme coordination and iron complexation by tyrosines can be excluded. The structure of the catalytic center remains to be elucidated by X-ray crystallography, but it can be predicted that the active site contains a mononuclear iron complex presumably consisting of histidines and carboxylic acid residues. Since then, corresponding enzymes have been obtained from *Drosophila melanogaster*,[64] mouse kidney,[65] and human intestine.[66]

Investigation of the substrate specificty of the enzyme revealed that any deviation from the rodlike structure of β-carotene is not tolerated by the enzyme, suggesting a rather rigid substrate binding pocket. Through interaction of hydrophobic amino acids with the methyl groups of β-carotene, the substrate is bound such that only the central double bond can be attacked.[67] Substrates with only one functional group in either carotenoid end group are cleaved; for example, cryptoxanthin **35** is cleaved to **33** and 3-hydroxy retinal **36**; α-carotene **37** is also accepted and cleaved in good yield to **33** and α-retinal **38**

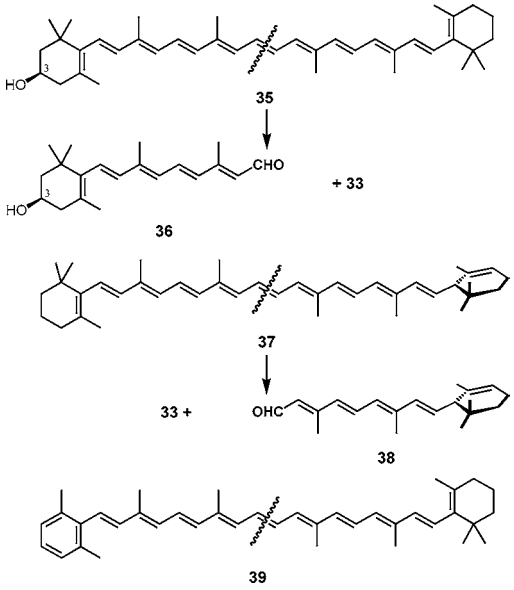

FIGURE 11. Enzymatic central cleavage of nonsymmetrical carotenoids.

(Figure 11). Further the nonnatural carotenoid Ph-β-carotene **39** was shown to be a substrate.

The discovery of these three nonsymmetric carotenoids proved to be important for determining the reaction mechanism of the enzyme-catalyzed central cleavage. It has already been mentioned that the enzyme was believed to belong to the class of dioxygenases, a conclusion based on weak experimental evidence.[68] We reasoned that it would be advantageous to employ a nonsymmetrical substrate yielding different aldehydes providing exact information of the incorporation of oxygen from water, air, or both into cleavage products. α-Carotene **37** was chosen as the best candidate because it was available isomerically pure and it was expected that the aldehydes **33** and **38** would behave similar in subsequent reactions required for MS analysis. To prevent the exchange of oxygen of the aldehydes[69] during incubation, a combined enzyme assay was used. Addition of HLADH (horse liver alcohol dehydrogenase) led to quantitative reduction of **33** and **38** in situ yielding the corresponding alcohols, which were immediately derivatized to give the silyl ethers suitable for GC-MS analysis. Incubation of **37** with the enzyme in 85% $^{17}O_2$ and 95% $H_2{}^{18}O$ revealed equal enrichment of the ^{17}O- and ^{18}O-label in both derivatives of metabolites **33** and **38**.[70] This result proves the incorporation of one ^{17}O atom of molecular oxygen and the concomitant incorporation of ^{18}O from labeled water. Accordingly, and in contrast to earlier belief, the reaction mechanism of enzymatic, central β-carotene cleavage is not in agreement with a dioxygenase-catalyzed procedure.

Note that a dioxygenase mechanism would require the [2+2] addition of $^{17}O_2$ to the central double bond of **37**, followed by fragmentation of the intermediate dioxetane yielding aldehydes labeled only with ^{17}O to the same extent; the incorporation of ^{18}O from water is not expected. Experimental evidence accounts for a monooxygenase-type mechanism (Figure 12) in which the first step is an

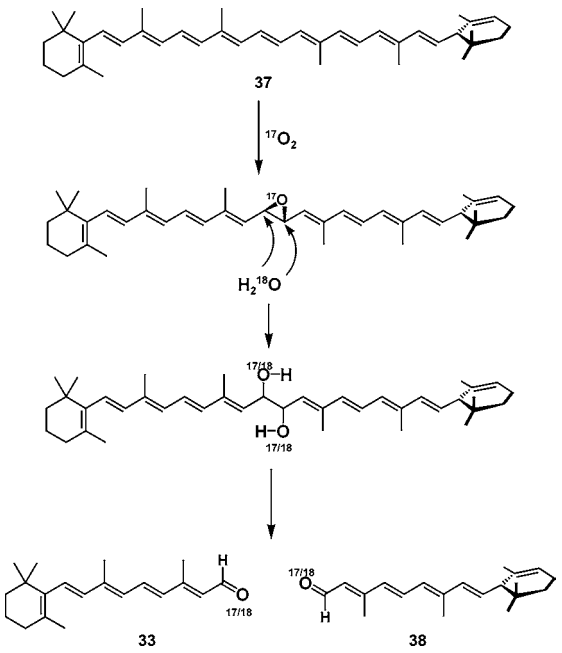

FIGURE 12. Enzymatic cleavage of α-carotene **37** in the presence of $^{17}O_2$ and $H_2{}^{18}O$.

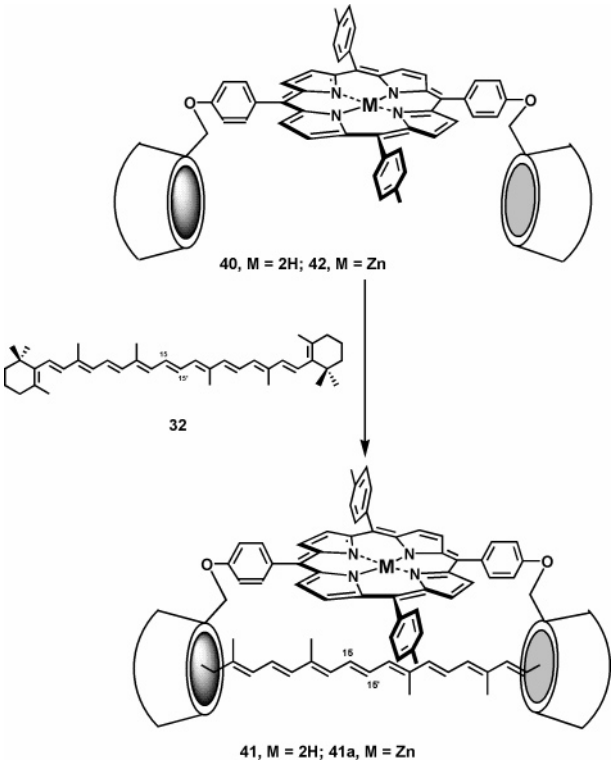

FIGURE 13. Binding of substrate **32** to the receptors **40**/**42**.

epoxidation of the central double bond of **37** followed by unselective ring opening by water and final diol cleavageto yield the aldehydes **33** and **38**. This sequence implies a high-valent non-heme oxoiron species as the reactive intermediate.

The fact that β-carotene 15,15′-monooxygenase controls the regiospecific cleavage of one C=C bond out of a possible six within the substrate is an intriguing and challenging one. To mimic such a regioselective system, the following strategy was employed: (i) synthesis of a receptor for which K_a of **32** is orders of magnitude greater than that for retinal **33** to prevent product inhibition; (ii) introduction of a reactive metal complex, which is capable of cleaving (*E*)-configured, conjugated double bonds to aldehydes; (iii) use of a co-oxidant that is inert toward **32** in the absence of the metal complex.

Disregarding the fact that the active site is a non-heme complex, the supramolecular system **40**, which consists of two β-cyclodextrin moieties linked by a porphyrin spacer, seemed to be an ideal candidate for the binding of **32** (Figure 13). Each of the cyclodextrins is capable of binding one of the cyclohexenoid endgroups of β-carotene, leaving the porphyrin to span the polyene chain. In the absence of **32**, several *unproductive* conformations of **40** are possible due to rotation about the ether linkages; in the presence of **32**, however, an *induced fit* should be observed yielding the inclusion complex **41**. As well as having the role of a spacer and potential metal ligand, the porphyrin in **40** is also useful for the determination of the binding constant, K_a, of **32** to **40**/**42**. Porphyrins display a characteristic fluorescence at around 600−650 nm, and the ability of carotenoids to quench this fluorescence was envisaged as a sensitive probe for the binding interaction of the two entities in an aqueous medium. From fluorescence quenching experiments, the binding constants were calculated for the free-base porphyrin, K_a(**32**→**40**) = 2.4 × 10^6 M^{-1}, and for the Zn porphyrin, K_a(**32**→**42**) = 8.3 × 10^6 M^{-1}.[71,72] This satisfied the first of our strategic criteria for mimicking the biological system because the binding constant for retinal **33** is smaller by 3 orders of magnitude. Accordingly product inhibition should not be observed if cleavage of the central double bond of **32** could be accomplished.

With regard to the choice of a metalloporphyrin capable of cleaving double bonds, a ruthenium porphyrin was chosen because preliminary experiments with (*E*,*E*)-1,4-diphenyl-1,3-butadiene, ruthenium tetraphenyl porphyrin/TBHP looked promising.[73] These experiments clearly showed that a O=Ru=O porphyrin is formed, which in contrast to compound I, see **3**, easily epoxidizes/cleaves (*E*)-configured conjugated double bonds. We have also tested the stability of **32** toward various co-oxidants; finally *tert*-butyl hydroperoxide (TBHP) was used, which showed no degradation of **32** within 24 h in the absence of catalyst.

With the above prerequisites satisfied, the stage was set to employ the supramolecular system **43** to investigate the catalytic cleavage of β-carotene **32** and Ph-β-carotene **39** (Figure 14). A biphasic system was established in which the substrates are extracted from a 9:1 mixture of hexane/chloroform into a water phase containing **43** (10 mol %) and TBHP. The reaction products, released from the receptor, are then extracted into the organic phase, aliquots of which were subjected to HPLC conditions developed for the analysis of enzymatic reactions.[67]

In contrast to **32**, which is mainly cleaved at the central C-15−15′ double bond but to a minor extent also at C(12′)=C(11′) and at C(10′)=C(9′), the cleavage of Ph-β-carotene **39** proceeded with regioselectivity since only retinal **33** and the corresponding Phe analogue **44** were

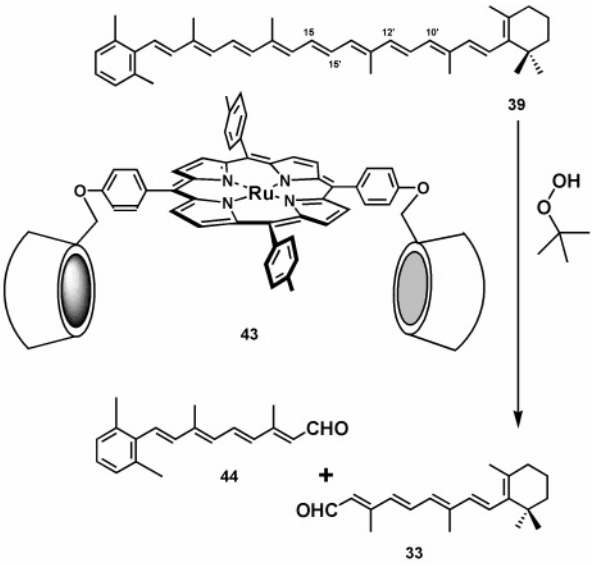

FIGURE 14. Central cleavage of Ph-β-carotene **39** catalyzed by the enzyme mimic **43**/TBHP.

detected.[72] This suggests that stronger hydrophobic interactions between the aromatic end-group of **39** and the β-cyclodextrin cavity are responsible for stabilizing the 1:1 inclusion complex with the central double bond under the reactive ruthenium center. In contrast, **32** slides within the inclusion complex exposing three double bonds rather than one to the reactive Ru=O. Determination of the binding constant of **39** to the receptor **40** supports this interpretation, that is, K_a(**39**→**40**) = 5.0×10^6 M^{-1} is about two times larger than K_a(**32**→**40**).[73] The combined yield of aldehydes **33** and **44** was 30%, which compares well with the efficiency of β-carotene 15,15′-monooxygenase, which gives retinal **32** in 20−25% yield.

The supramolecular system presented here is one of the few examples that mimics the reactivity and selectivity of an enzymatic reaction using unmodified, original substrates of an enzyme.

V Conclusions

When the three enzymes discussed here were discovered in nature, it seemed nearly impossible to pursue most of the reactions catalyzed by these proteins. This Account, as well as contributions from many other groups, demonstrates the value of synthetic active site analogues/enzyme models to improve our understanding of enzymatic catalysis. This approach, however, to reduce the protein to its center of chemical reactivity obviously has inherent disadvantages. In particular, there is no simple way to mimic the substrate binding site and its structural flexibility during catalysis. It is also evident from available X-ray structures (see P450 and CPO) that amino acids from the distal binding sites participate in catalysis by providing protons, stabilizing catalytically competent intermediates, supporting electron transport from redox proteins, and hence in general contributing to the chemical diversity of an otherwise rather uniform cofactor. Last, but not least, amino acids of the substrate binding domain specifically orient the substrate for regio- and stereoselective reactions. In part, this can be synthetically mimicked by receptor subunits such as cyclodextrins, crown ethers, or calixarenes. In general, these artificial systems display an invariant binding site with residual flexibility, which rarely can be tuned or optimized to approach the selectivity of the protein−substrate interactions. This is obvious especially regarding the P450-catalyzed hydroxylation of nonactivated C−H bonds. We have been able to show[74] that this reaction can be done intramolecularly using **12** and PhIO or $^{18}O_2$, but it has been impossible until now to pursue this oxidation in an intermolecular fashion even if potential biding sites are attached to the distal site of the porphyrin, see **16**. These results indicate the significance of an entropic contribution to reactivity/catalysis, that is, the substrate must be positioned such that the C−H bond is in binding distance to O=Fe(IV). Thus it seems that the lack of control regarding suitable substrate orientation is the major obstacle of (many) artificial enzyme systems. This problem could be overcome taking advantage of information available from antibody−antigen interactions; if one could combine cofactor reactivity with suitable small protein fragments containing the antigen/substrate binding site, one may approach reactivity and catalytic turnover close to natural enzymes.

This work was generously supported by the Swiss National Science Foundation and F. Hoffmann-La Roche Ltd. (Vitamins & Fine Chemicals Division). I am also very grateful to my co-workers, mentioned in the references.

References

(1) Woggon, W.-D. Cytochrome P450: Significance, Reaction Mechanisms and Active Site Analogues. *Top. Curr. Chem.* **1997**, *184*, 39−96.
(2) Flinspach, M.; Li, H.; Jamal, J.; Yang, W.; Huang, H.; Silverman, R. B.; Poulos, T. L. Structures of the Neuronal and Endothelial Nitrici Oxide Synthase Heme Domain with D-Nitroarginine-conatining Dipeptide Inhibitors Bound. *Biochemistry* **2004**, *43*, 5181−5187.
(3) Roman, L. J.; Martasek, P.; Masters, B. S. S. Intrinsic and Extrinsic Modulation of Nitric Oxide Synthase Activity. *Chem. Rev.* **2002**, *102*, 1179−1189.
(4) Marletta, A. M.; Hurshman, A. R.; Rusche, K. M. Catalysis by Nitric Oxide Synthase. *Curr. Opin. Chem. Biol.* **1998**, *2*, 656−663.
(5) Franssen, M. C. R. Halogenation and Oxidation Reactions with Haloperoxidases. *Biocatalysis* **1994**, *10*, 87−111.
(6) Libby, R. D.; Beachy, T. M.; Phipps, A. K. Quantitating Direct Chlorine Transfer From Enzyme to Substrate in Chlorperoxidase-catalyzed Reactions. *J. Biol. Chem.* **1996**, *271*, 21820−21827.
(7) Dawson, J. H.; Sono, M. Cytochrome P-450 and Chloroperoxidase: Thiolate-Ligated Heme Enzymes. Spectroscopic Determination of Their Active Site Structures and mechanistic Implications of Thiolate ligation. *Chem. Rev.* **1987**, *87*, 1255−1276.
(8) Sono, M.; Roach, M. P.; Coulter, E. D.; Dawson, J. H. Heme-Containing Oxygenases. *Chem. Rev.* **1996**, *96*, 2841−2887.
(9) Unger, B. P.; Gunsalus, I. C.; Sligar, S. G. Nucleotide Sequence of the Pseudomonas Putida Cytochrome $P450_{cam}$ Gene and its Expression in *Escherichia coli*. *J. Biol. Chem.* **1986**, *261*, 1158−1163.
(10) Poulos, T. L.; Finzel, B. C.; Gunsalus, I. C.; Wagner, G. C.; Kraut, J. The 2.6-Å Crystal Structure of *Pseudomonas putida* Cytochrome P-450. *J. Biol. Chem.* **1985**, *260*, 6122−6130.
(11) Poulos, T. L.; Finzel, B. C.; Howard, A. J. Crystal Structure of Substrate-free *Pseudomonas putida* Cytochrome P-450. *Biochemistry* **1986**, *25*, 5314−5322.
(12) Poulos, T. L.; Finzel, B. C.; Howard, A. J. High-Resolution Crystal Structure of Cytochrome $P450_{cam}$. *J. Mol. Biol.* **1987**, *195*, 687−700.
(13) Raag, R.; Poulos, T. L. The Structural Basis for Substrate-Induced Changes in Redox potential and Spin Equilibrium in Cytochrome $P\text{-}450_{cam}$. *Biochemistry* **1989**, *28*, 917−922.

(14) Raag, R.; Poulos, T. L. Crystal Structure of Carbon Monoxide−Substrate−Cytochrome P-450$_{cam}$ Ternary Complex. *Biochemistry* **1989**, *28*, 7586−7592.

(15) Raag, R.; Poulos, T. L. Crystal Structure of Cytochrome P-450$_{cam}$ Complexed with Camphane, Thiocamphor and Adamantane: Factors Controlling P-450 Substrate Hydroxylation. *Biochemistry* **1991** *30*, 2674−2684.

(16) Schlichting, I.; Berendzen, J.; Chu, K.; Stock, A. M.; Maves, S. A.; Benson, D. E.; Sweet, R. M.; Ringe, D.; Petsko, G. A.; Sligar, S. G. The Catalytic Pathway of Cytochrome P450cam at Atomic Resolution. *Science* **2000**, *287*, 1615−1622.

(17) Davydov, R.; Makris, T. M.; Kofman, V.; Werst, D. E.; Sligar, S. G.; Hoffman, B. M. Hydroxylation of Camphor by Reduced Oxy-Cytochrome P450$_{cam}$: Mechanistic Implications of EPR and ENDOR Studies of Catalytic Intermediates in Native and Mutant Enzymes. *J. Am. Chem. Soc.* **2001**, *123*, 1403−1415.

(18) Ogliaro, F.; Shimrit, C.; de Visser, S. P.; Shaik, S. Medium Polarization and Hydrogen Bonding Effects on Compound I of Cytochrome P450: What Kind of a Radical Is It Really? *J. Am. Chem. Soc.* **2000**, *122*, 12892−12893.

(19) Green, M. T. Evidence for Sulfur-Based Radicals in Thiolate Compound I Intermediates. *J. Am. Chem. Soc.* **1999**, *121*, 7939−7940.

(20) Green, M. T. Role of the Axial Ligand in Determining the Spin State of Resting Cytochrome P450. *J. Am. Chem. Soc.* **1998**, *120*, 10772−10773.

(21) Harris, D.; Loew, G. H. Determinants of the Spin State of the Resting State of Cytochrome P450$_{cam}$. *J. Am. Chem. Soc.* **1993**, *115*, 8775−8779.

(22) Newcomb, M.; Toy, P. H. Hypersensitive Radical Probes and the Mechanism of Cytochrome P450−Catalyzed Reactions. *Acc. Chem. Res.* **2000**, *33*, 449−455.

(23) Shaik, S.; Filatov, M.; Schröder, D.; Schwarz, H. Electronic Structure Makes a Difference: P450-mediated Hydroxylations as a Two-State Reactivity Paradigm. *Chem.—Eur. J.* **1998**, *4*, 193−199.

(24) Ogliaro, F.; Nathan, H.; Cohen, S.; Filatov, M.; deVisser, S. P.; Shaik, S. Ar Rebound Mechanism of Hydroxylation by Cytochrome P450: Stepwise and Effectively Concerted Pathways and Their Reactivity Patterns. *J. Am. Chem. Soc.* **2000**, *122*, 8977−8989.

(25) Dawson, J. H.; Sono, M. Cytochrome P-450 and Chloroperoxidase: Thiolate-Ligated Heme Enzymes. Spectroscopic Determination of Their Active Site Structures and mechanistic Implications of Thiolate ligation. *Chem. Rev.* **1987**, *87*, 1255−1276 and references therein.

(26) Omura, T.; Sato, R. The Carbon Monoxide-Binding Pigment of Liver Microsomes. I. Evidence for its Hemoprotein Nature. *J. Biol. Chem.* **1964**, *239*, 2370−2378.

(27) Green, M. T.; Dawson, J. H.; Gray, H. B. Oxoiro(IV) in Chloroperoxidase Compound II is Basic: Implication for P450 Chemistry. *Science* **2004**, *304*, 1653−1656.

(28) Sligar, S. G.; Gunsalus, I. C. A Thermodynamic Model Regulation: Modulation of Redox Equilibria in Camphor Monoxygenase. *Proc. Natl. Acad. Sci. U.S.A.* **1976**, *73*, 1078−1082.

(29) Hintz, M. J.; Peterson, J. A. The Kinetics of Reduction of Cytochrome P-450cam by Reduced Putidaredoxin. *J. Biol. Chem.* **1981**, *25*, 6721−6728.

(30) Hintz, M. J.; Mock, D. M.; Peterson, L. L.; Tuttle, K.; Peterson, J. A. Equilibrium and Kinetics Studies of the Interaction of Cytochrome P-450$_{cam}$ and Putidaredoxin. *J. Biol. Chem.* **1982**, *25*, 14324−14332.

(31) Honeychurch, M. J.; Hill, H. A. O.; Wong, L.-L. The Thermodynamics and Kinetics of Electron Transfer in the Cytochrome P450$_{cam}$ Enzyme System. *FEBS Lett.* **1999**, *451*, 351−353.

(32) Sigfridsson, E.; Olsson, M. H. M.; Ryde, U. A Comparison of the Inner-Sphere Reorganization Energies of Cytochromes, Iron−Sulfur Clusters, and Blue Copper Proteins. *J. Phys. Chem. B* **2001**, *105*, 5546−5552.

(33) Unno, M.; Christian, J. F.; Sjodin, T.; Benson, D. E.; Macdonald, I. D. G.; Sligar, S. G.; Champion, P. M. Complex Formation of Cytochrome P450$_{cam}$ with Putidaredoxin. *J. Biol. Chem.* **2002**, *277*, 2547−2553.

(34) Tosha, T.; Yoshioka, S.; Ishimori, K.; Morishima, I. L358P Mutation on Cytochrome P450$_{cam}$ Simulates Structural Changes upon Putidaredoxin Binding. *J. Biol. Chem.* **2004**, *279*, 42836−42843.

(35) Nagano, S.; Tosha, T.; Yoshioka, S.; Ishimori, K.; Morishima, I. Crystal Structure of the Cytochrome P450$_{cam}$ Mutant That Exhibits the Same Spectral Perturbations Induced by Putidaredoxin Binding. *J. Biol. Chem.* **2004**, *279*, 42844−42849.

(36) Poulos, T. L. The role of the Proximal Ligand in Heme Enzymes. *J. Biol. Inorg. Chem.* **1996**, *1*, 356−359.

(37) Stäubli, B.; Fretz, H.; Piantini, U.; Woggon, W.-D. Synthetic Models of the Active Site of Cytoxchrome P450; The Synthesis of a Doubly-Bridged Iron(II) porphyrin Carrying a Tightly Bound Thiolate Ligand. *Helv. Chim. Acta* **1987**, *70*, 1173−1193.

(38) Ghirlanda, S. L. Ph.D. Thesis, University of Zurich, 1994.

(39) Makino, R.; Chiang, R.; Hager, L. P. Oxidation−Reduction Potential Measurements on Chloroperoxidase and its Complexes. *Biochemistry* **1976**, *15*, 4748−4754.

(40) Kozuch, S.; Leifels, T.; Shaik, S.; Woggon, W.-D. Synthetic Models of Cytochrome P450 Enzyme: How Different are They from the Natural Species? submitted for publication.

(41) Wagenknecht, H.-A.; Claude, C.; Woggon, W.-D. New Enzyme Models of Chloroperoxidase: Improved Stability and Catalytic Efficiency of Iron Porphyrinates Containing a Thiolato Ligand. *Helv. Chim. Acta* **1998**, *81*, 1506−1520.

(42) Aissaoui, H.; Ghirlanda, S. L.; Gmür, C.; Woggon, W.-D. The Synthesis of a New Active-Site Analogue of Cytochrome P450 Carrying Substrate Recognition Sites and a Thiolate Ligand. *J. Mol. Catal.* **1996**, *113*, 393−402.

(43) Furrer, O. Ph.D. Thesis, University of Basel, 1998.

(44) Ueyama, N.; Nishikawa, N.; Yamada, Y.; Okamura, T.-A.; Nakamura, A. Cytochrome P450 Model (Porpphyrinato) (thiolato) iron-(III) Complexes with Single and Double NH···S Hydrogen Bonds at the Thiolate Site. *J. Am. Chem. Soc.* **1996**, *118*, 12826−12827.

(45) Thomann, H.; Bernardo, M.; Goldfarb, D.; Kroneck, P. M. H.; Ullrich, V. Evidence for Water Binding to the Fe Center in Cytochrome P450$_{cam}$ Obtained by ^{17}O Electron Spin−Echo Envelope Modulation Spectroscopy. *J. Am. Chem. Soc.* **1995**, *117*, 8243−8251.

(46) Aissaoui, H.; Bachmann, R.; Schweiger, A.; Woggon, W.-D. On the Origin of the Low-Spin Character of Cytochrome P450cam in the Resting State − Investigations of Enzyme Models with Pulse EPR and ENDOR Spectroscopy. *Angew. Chem., Int. Ed.* **1998**, *37*, 2998−3002.

(47) Lochner, M.; Meuwly, M.; Woggon, W.-D. The Origin of the Low-spin Character of the Resting State of Cytochrome P450$_{cam}$ Investigated by Means of Active Site Analogues. *Chem. Commun.* **2003**, 1330−1332.

(48) Lochner, M.; Mu, L.; Woggon, W.-D. Remote Effects Modulating the Spin Equilibrium of the Resting State of Cytochrome P450$_{cam}$ − an Investigation Using Active Site Analogues, *Adv. Synth. Catal.* **2003**, *345*, 743−765.

(49) Comte, C.; Gros, C. P.; Koeller, S.; Guilard, R.; Nurco, D. J.; Smith, K. M. Synthesis and Characterization of a Novel Series of bis-linked Diaza-18-crown-6 porphyrins. *New J. Chem.* **1998**, 621−626.

(50) Morris, D. R.; Hager, L. P. Chloroperoxidase I. Isolation and Properties of the Crystalline Glycoprotein. *J. Biol. Chem.* **1966**, *241*, 1763−1768.

(51) Libby, R. D.; Shedd, A. L.; Phipps, A. K.; Beachy, T. M.; Gerstberger, S. M. Defining the Involvement of Hypochlorous Acid or Chlorine as Enzyme-generated Intermediates in Chloroperoxidase-catalyzed Reactions. *J. Biol. Chem.* **1992**, *267*, 1769−1775.

(52) Wagenknecht, H.-A.; Woggon, W.-D. New Active-Site Analogues of Chloroperoxidase-Syntheses and Catalytic Reactions. *Angew. Chem., Int. Ed. Engl.* **1997**, *36*, 390−392.

(53) Wagenknecht, H.-A.; Woggon, W.-D. Identification of Intermediates in the Catalytic Cycle of Chloroperoxidase. *Chem. Biol.* **1997**, *4*, 367−372.

(54) Sundaramoorthy, M.; Terner, J.; Poulos, T. L. The Crystal Structure of Chloroperoxidase: a Heme Peroxidase-Cytochrome P450 Functional Hybrid. *Structure* **1995**, *3*, 1367−1377.

(55) Blanke, S. R.; Hager, L. P. Chemical Modification of Chloroperoxidase With Diethylpyrocarbonate. Evidence for the Presence of an Essential Histidine Residue. *J. Biol. Chem.* **1990**, *265*, 12454−2461.

(56) Sundaramoorthy, M.; Terner, J.; Poulos, T. L. Stereochemistry of the Chloroperoxidase Active Site: Crystallographic and Molecular-Modeling Studies. *Chem. Biol.* **1998**, *5*, 461−473.

(57) Britton, G. The Biosynthesis of Carotenoids: a Progress Report. *Pure Appl. Chem.* **1991**, *63*, 101−108.

(58) Rohmer, M. The Mevaolnate-dependent Methylerythritol 4-phosphate (MEP) Pathway for Isoprenoid Biosynthesis, Including Carotenoids. *Pure Appl. Chem.* **1999**, *71*, 2279−2284.

(59) Edge, R.; McGarvey, D. J.; Truscott, T. G. The Carotenoids as Antioxidants − a Review. *J. Photochem. Photobiol., B* **1997**, *41*, 189−200.

(60) Olson, J. A.; Hayaishi, O. The Enzymatic Cleavage of β-Carotene Into Vitamin A by Soluble Enzymes of Rat Liver and Intestine. *Proc. Natl. Acad. Sci. U.S.A.* **1965**, *54*, 1364−1370.

(61) Wang, X. D.; Tang, G. W.; Fox, J. G.; Krinsky, N. I.; Russell, R. M. Enzymatic Conversion of β-Carotene Into β-apo-Carotenals and Retinoids by Human, Monkey, Ferret, and Rat Tissues. *Arch. Biochem. Biophys.* **1991**, *285*, 8−16.

(62) Wyss, A.; Wirtz, G.; Woggon, W.-D.; Brugger, R.; Wyss, M.; Friedlein, A.; Bachmann, H.; Hunziker, W. Cloning and Expression of β-Carotene 15,15′-Dioxygenase. *Biochem. Biophys. Res. Commun.* **2000**, *27*, 334−336.
(63) Wyss, A.; Wirtz, G. M.; Woggon, W.-D.; Brugger, R.; Wyss, M.; Friedlein, A.; Riss, G.; Bachmann, H.; Hunziker, W. Expression Pattern and Localization of β-Carotene 15,15′-Dioxygenase in Different Tissues. *Biochem. J.* **2001**, *354*, 521−529.
(64) Von Lintig, J.; Vogt, K. Filling the Gap in Vitamin A Research. Molecular Identification of an Enzyme Cleaving β-Carotene to Retinal. *J. Biol. Chem.* **2000**, *275*, 11915−11920.
(65) Paik, J.; During, A.; Harrison, E. H.; Mendelsohn, C. L.; Lai, K.; Blaner, W. S. Expression and Characterization of a Murine Enzyme Able to Cleave β-Carotene. The Formation of Retinoids. *J. Biol. Chem.* **2001**, *276*, 32160−32168.
(66) Lindqvist, A.; Andersson, S. Biochemical Properties of Purified Recombinant Human β-Carotene 15,15′-Monooxygenase. *J. Biol. Chem.* **2002**, *277*, 23942−23948.
(67) Wirtz, G. M.; Bornemann, C.; Giger, A.; Muller, R. K.; Schneider, H.; Schlotterbeck, G.; Schiefer, G.; Woggon, W.-D. The Substrate Specificity of β-Carotene 15,15′-Monooxygenase. *Helv. Chim. Acta* **2001**, *84*, 2301−2315.
(68) Vartapetyan, B. B.; Dmitrovskii, A. A.; Alkhazov, D. G.; Lemberg, I. Kh.; Girshin, A. B.; Gusinskii, G. M.; Starikova, N. A.; Erofeeva, N. N.; Bogdanova, I. P. A New Approach to the Study of the Mechanism ofVitamin A Biosynthesis from Carotene. Oxygen-18 Activation by Nuclear Reaction 18O(α, n, γ)21Ne Using Cyclotron-accelerated α-Particles. *Biokhimiya (Moscow)* **1966**, *31*, 881−886.
(69) Retey, J.; Umani-Ronchi, A.; Seibl, J.; Arigoni, D. Mechanisms of the Propanediol Dehydratase Reaction. *Experientia* **1966**, *22*, 502−503.
(70) Leuenberger, M. G.; Engeloch-Jarret, C.; Woggon, W.-D. The Reaction Mechanism of the Enzyme-catalyzed Central Cleavage of β-Carotene in Retinal. *Angew. Chem., Int. Ed.* **2001**, *40*, 2614−2617.
(71) French, R. R.; Wirz, J.; Woggon, W.-D. A Synthetic Receptor for β-Carotene. Towards an Enzyme Mimic for Central Cleavage. *Helv. Chim. Acta* **1998**, *81*, 1521−1527.
(72) French, R. R.; Holzer, P.; Leuenberger, M. G.; Woggon, W.-D. A Supramolecular Enzyme Mimic That Catalyzes the 15,15′ Double Bond Scission of β,β-Carotene, *Angew. Chem., Int. Ed.* **2000**, *39*, 1267−1269.
(73) French, R. R.; Holzer, P.; Leuenberger, M.; Nold, M. C.; Woggon, W.-D. A Supramolecular Enzyme Model Catalyzing the Central Cleavage of Carotenoids. *J. Inorg. Biochem.* **2002**, *88*, 295−304.
(74) Patzelt, H; Woggon, W.-D. Oxygen Insertion into Nonactivated Carbon−Hydrogen Bonds: the First Observation of O_2 Cleavage by a P-450 Enzyme Model in the Presence of a Thiolate Ligand. *Helv. Chim. Acta* **1992**, *75*, 523−530.

AR0400793